

Learning Disentangled Intent Representations for Zero-shot Intent Detection

Qingyi Si,^{1,2} Yuanxin Liu,^{1,2} Peng Fu¹ Jiangnan Li^{1,2} Zheng Lin¹ Weiping Wang¹

¹ Institute of Information Engineering, Chinese Academy of Sciences, Beijing, China

¹ School of Cyber Security, University of Chinese Academy of Sciences, Beijing, China
{siqingyi,liuyuanxin,fupeng,lijiangnan,linzheng,wangweiping}@iie.ac.cn

Abstract

Zero-shot intent detection (ZSID) aims to deal with the continuously emerging intents without annotated training data. However, existing ZSID systems suffer from two limitations: 1) They are not good at modeling the relationship between seen and unseen intents, when the label names are given in the form of raw phrases or sentences. 2) They cannot effectively recognize unseen intents under the generalized intent detection (GZSID) setting. A critical factor behind these limitations is the representations of unseen intents, which cannot be learned in the training stage. To address this problem, we propose a class-transductive framework that utilizes unseen class labels to learn **Disentangled Intent Representations (DIR)**. Specifically, we allow the model to predict unseen intents in the training stage, with the corresponding label names serving as input utterances. Under this framework, we introduce a multi-task learning objective, which encourages the model to learn the distinctions among intents, and a similarity scorer, which estimates the connections among intents more accurately based on the learned intent representations. Since the purpose of DIR is to provide better intent representations, it can be easily integrated with existing ZSID and GZSID methods. Experiments on two real-world datasets show that the proposed framework brings consistent improvement to the baseline systems, regardless of the model architectures or zero-shot learning strategies.

Introduction

In recent years, smart devices with built-in personal assistants like Google Assistant and Siri are becoming omnipresent. Behind these intelligent systems, a key question is how to identify the underlying intent of a user utterance, which has triggered a large amount of work on intent detection (Hu et al. 2009; Tur et al. 2012; Xu and Sarikaya 2013; Ravuri and Stolcke 2015; Liu and Lane 2016; Nam, Mencía, and Fürnkranz 2016). Most existing intent detection systems are built on deep learning models trained on large-scale annotated data. However, as user demands and the functions of smart devices continue to grow, collecting supervised data for every new intent becomes time-consuming and labor-intensive.

To address this issue, some studies tackle intent detection in the zero-shot learning (ZSL) manner, attempting to utilize the learned knowledge of seen classes to help detect unseen classes. The recent methods of zero-shot intent detection

(ZSID) can be roughly divided into two categories: The first category (Xia et al. 2018; Liu et al. 2019), referred to as the transformation-based methods, utilizes word embeddings of label names to establish a similarity matrix, which is then used to transfer the prediction space of seen intents to unseen intents. Another line of work is based on the compatibility-based methods (Chen, Hakkani-Tür, and He 2016; Kumar et al. 2017), which aims to encode the label names and utterances into representations in the same semantic space and then calculate their similarity. In both kinds of methods, a critical problem is learning intent representations. However, most existing ZSID methods are class-inductive, which relies entirely on labeled data from seen intents in the training stage. Consequently, the representations of unseen intents cannot be learned, resulting in two limitations.

First, the ZSID methods are not good at modeling the relationship between seen and unseen intents. For the transformation-based methods, when the label names are given in the form of raw phrases or sentences, word embeddings of label names are inadequate to associate the connections between seen and unseen intents. For example, “BookRestaurant” is similar to “RateBook” when measured by word embeddings, as they share the word “Book” (Appendix A shows the similarity matrix). However, the meaning of these two intents are not that relevant. For the compatibility-based methods, they minimize the similarity between seen intent samples and seen label names in a shared semantic space, and directly transfer it to detect unseen intents. Since the unseen intent representations are not learned, they might be entangled with the representations of seen intents. This can severely hurt the accuracy of the predicted label-utterance similarity, especially when the expressions of utterances are diverse.

Second, the vanilla ZSL methods are not applicable to generalized intent detection (GZSID). Compared with the ZSL setting (Lampert, Nickisch, and Harmeling 2009), which assumes that the models are only presented with utterances from unseen classes at test time, GZSID requires the model to detect both seen and unseen intents. In GZSID, existing ZSL models usually suffer from the dubbed domain shift (Fu et al. 2015a) problem, in which utterances from unseen intents are almost always mistakenly classified into seen intents.

Unlike the class-inductive methods, class-transductive

ZSL uses semantic information about the unseen classes for model training (Wang et al. 2019; Xian et al. 2019). In the context of intent detection, the label name provides a proper sketch of the intent meaning. Motivated by this, we propose to utilize label names of the unseen intents to learn disentangled intent representations (DIR). Specifically, we include the unseen intents into the prediction space during training, with the label names serving as the pseudo utterances. This allows the model to learn the boundary of each seen and unseen class in the semantic space. Under this framework, we introduce an assistant task that forces the model to find the distinction between seen and unseen intents, thereby alleviating the domain-shift problem. On this basis, we refine the word embedding based similarity matrix by averaging the representations of all corresponding (seen intent) utterances and (unseen intent) label names. As a result, we can better capture the intent meanings and the similarity matrix reflects more accurate intent connections.

In summary, our contribution is three-fold:

- In response to the limitations of existing ZSID systems, we propose a class-transductive framework that utilizes unseen intent label names to learn disentangled intent representations. To the best of our knowledge, this work is the first testament to the effectiveness of class-transductive ZSL methods in intent detection.
- Under the framework, we present a multi-task learning objective to find the inter-intent distinctions and a similarity scorer to associate the inter-intent connections.
- Empirical results on ZSID and GZSDI in two benchmarks show that DIR can bring improvement to wide range of ZSID systems with different zero-shot learning strategies and model architectures.

We believe that the potential of class-transductive ZSL in intent detection is still not fully exploited, to encourage more related studies in the future, we will release our codes and data.

Related Work

Intent Detection In recent years, deep neural network based methods are showing great success in intent detection (Hu et al. 2009; Xu and Sarikaya 2013; Zhang et al. 2016a; Liu and Lane 2016; Chen et al. 2016; Zhang et al. 2019; Haihong et al. 2019). However, their success primarily relies on large amount of annotated data.

Zero-shot Learning Zero-shot learning, as proposed by Lampert, Nickisch, and Harmeling (2009), requires the models to distinguish among unseen classes without annotated data. In computer vision, ZSL is a well-developed sub-field, where a common approach is to relate unseen classes with seen classes through visual attributes (Farhadi et al. 2009; Parikh and Grauman 2011) or word2vec representations of the class names (Mikolov et al. 2013; Frome et al. 2013; Socher et al. 2013). Inspired by these methods, Xia et al. (2018); Liu et al. (2019) calculate the inter-intent similarity based on the word embeddings of intent labels. The similarity scores are then used to transform the predictions from seen intents to unseen intents. Compatibility models

(Chen, Hakkani-Tür, and He 2016; Kumar et al. 2017) attempt to learn a shared semantic space for label names and utterances, and then perform intent detection by measuring the intent-utterance similarity in this space. There are also studies resorting to external knowledge, e.g., label ontologies (Ferreira, Jabaian, and Lefevre 2015; Ferreira, Jabaian, and Lefèvre 2015) or human-defined attributes (Yazdani and Henderson 2015; Zhang, Lertvittayakumjorn, and Guo 2019), which, however, are laborious to obtain.

Generalized Zero-shot Learning Frome et al. (2013); Norouzi et al. (2014); Mensink et al. (2012) extended ZSL by including seen classes into the prediction space at test time. However, the test samples still only come from unseen classes. In contrast, Scheirer et al. (2012) allowed test sample to come from seen classes. CMT (Socher et al. 2013) proposed a two-stage procedure for GZSL, which first determines whether a test sample belongs to seen classes or unseen classes, and then apply the corresponding classifier. Similarly, Zhang et al. (2016b) estimated the probability of each sample coming from an unseen class. In the task of intent detection, ReCapsNet-ZS (Liu et al. 2019) enhanced IntentCapsNet (Xia et al. 2018) in GZSID by modeling the correlation between the dimensions of word embeddings, which can find a more accurate connection between seen and unseen intents. On the basis of ReCapsNet-ZS, Yan et al. (2020) proposed a two-stage GZSID method that combines unknown intent detection (UID) (Lin and Xu 2019) and ZSID, which successfully resolves the domain-shift problem. However, this is at the cost of the performance in seen intents, which is the majority in real-world applications.

Class-transductive Zero-shot Learning Class-transductive zero-shot learning utilizes semantic information (typically a textual description) about the unseen classes in the training stage. In the CV field, class-transductive methods are used to infer the relationship between seen and unseen classes (Fu et al. 2015b, 2018) or directly predict the parameters of unseen intent classifiers (Elhoseiny, Saleh, and Elgammal 2013; Wang, Ye, and Gupta 2018). In comparison, DIR uses the unseen label names as training instances to learn unseen intent representations, which takes advantage of the fact that intent label names and utterances both come from the textual domain.

Problem Formulation

Zero-shot Intent Detection In ZSID, the model is trained on the annotated dataset $\{(x, y)\}$, where $y \in Y_{seen} = \{y_1^s, y_2^s, \dots, y_J^s\}$ is the intent label and x is the utterance. At test time, the goal is to identify the intent of an utterance, which belongs to one of the J unseen intents $Y_{unseen} = \{y_1^u, y_2^u, \dots, y_J^u\}$, where $Y_{seen} \cap Y_{unseen} = \emptyset$.

Generalized Zero-shot Intent Detection In GZSID, the model is presented with utterances from either seen or unseen intents, and the prediction space is $Y_{seen} \cup Y_{unseen}$.

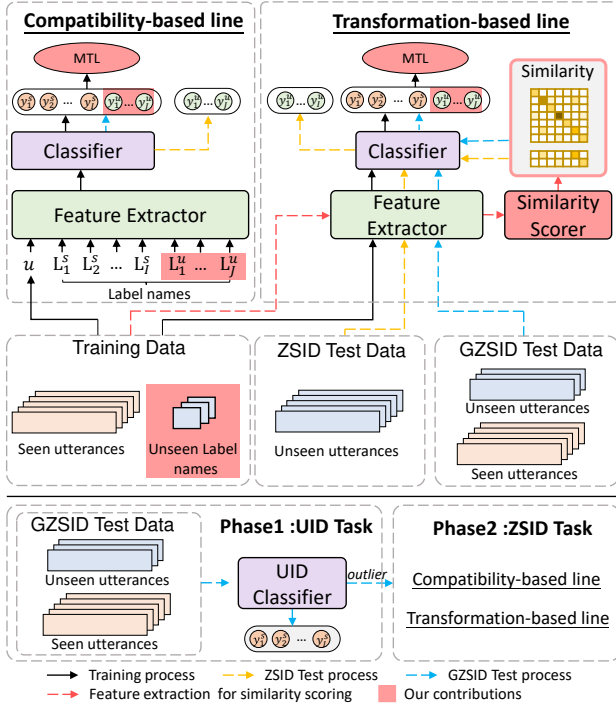


Figure 1: Illustration of how to integrate compatibility-based method (upper left), transformation-based method (upper right) and two-stage GZSID method (lower) with DIR.

Unknown Intent Detection (UID) (Lin and Xu 2019) In UID, the training set is the same as ZSID and GZSID. During testing, the model is expected to decide whether an utterance belongs to the unknown intents. The prediction space is $\{y_1^s, y_2^s, \dots, y_j^s, y_{unseen}\}$, where all the unknown intents are grouped into a single class y_{unseen} .

Simplified Unknown Intent Detection (SUID) The prediction space is reduced to $\{y_{seen}, y_{unseen}\}$ in SUID. In our multi-task learning, SUID serves as an assistant task.

Disentangled Intent Representation Framework

Figure 1 gives an overview of our DIR framework. The core idea is to expand the prediction space in the training stage to include unseen classes, with the unseen label names serving as pseudo utterances. During test time, the trained model can be applied to both ZSID and GZSID settings. Next, we will describe how to integrate DIR into transformation-based, compatibility-based methods and the two-stage GZSID method respectively.

Transformation-based Methods

Feature Extractor The feature extractor transforms an input text into a sequence of hidden vectors $\mathbf{H} = (\mathbf{h}_1, \mathbf{h}_2, \dots, \mathbf{h}_T) \in \mathbb{R}^{T \times D_H}$, where D_H is the hidden dimension and T is the sequence length. The text representation is then obtained by averaging over the T hidden vec-

tors. Note that the architecture of feature extractor is a free choice in DIR framework. Specially, on top of the \mathbf{H} produced by a Bi-LSTM (Schuster and Paliwal 1997), IntentCapsNet (Xia et al. 2018) applies a multi-head attention layer (Vaswani et al. 2017; Lin et al. 2017). Each attention head represents a unique semantic feature, which gives rise to $\{\mathbf{m}_1, \mathbf{m}_2, \dots, \mathbf{m}_R\} \in \mathbb{R}^{R \times D_H}$, where R is the number of attention heads. We follow this operation when combining IntentCapsNet with DIR.

Intent Classifier There are two commonly used classifiers in intent detection: 1) the linear classifier and 2) the capsule networks (Sabour, Frosst, and Hinton 2017). The linear classifier predicts the intent probabilities as:

$$\mathbf{v}_{tr} = \text{Softmax}\left(\frac{1}{T} \sum_{t=1:T} \mathbf{h}_t\right) \mathbf{W} \quad (1)$$

where $\mathbf{W} \in \mathbb{R}^{D_H \times K}$ is the weight matrix, and $K = I + J$ is the total number of seen and unseen classes. In capsule networks, the Dynamic Routing algorithm (Sabour, Frosst, and Hinton 2017) is used to aggregate the low-level features $\{\mathbf{m}_1, \mathbf{m}_2, \dots, \mathbf{m}_R\}$ into higher-level representations:

$$\begin{aligned} \hat{\mathbf{u}}_{k|r} &= \mathbf{m}_r \mathbf{W}_{k,r} \\ \mathbf{s}_k &= \sum_r c_{kr} \hat{\mathbf{u}}_{k|r} \end{aligned} \quad (2)$$

where c_{kr} is the coefficient that determines how much the r^{th} semantic feature contributes to intent y_k . Following \mathbf{s}_k is the squash function, which gives rise to the activation vectors $\mathbf{V} = (\mathbf{v}_1, \mathbf{v}_2, \dots, \mathbf{v}_K)$. The 2-norms of these vectors are used as the probability of different intent classes.

Multi-task Learning Objective The assistant task SUID has two class labels, namely y_{seen} and y_{unseen} . If an utterance x belongs to one of the seen classes, then x is labeled as y_{seen} in SUID, and otherwise x is labeled as y_{unseen} . In order to compute the probabilities for y_{seen} and y_{unseen} , we sum up the probabilities of all intent classes in the respective categories. For linear classifiers, we compute the sum of the first I dimensions of the vector \mathbf{v}_{tr} for y_{seen} and the last J dimensions for y_{unseen} . For capsule networks, we sum up the 2-norms of the activation vectors $(\mathbf{v}_1, \mathbf{v}_2, \dots, \mathbf{v}_I)$ and $(\mathbf{v}_{I+1}, \mathbf{v}_{I+2}, \dots, \mathbf{v}_K)$, respectively.

Then, linear classifier is trained with cross-entropy loss, which is formulated as:

$$\mathcal{L}_{cross} = \sum_{k=1}^K z_k \log(p_k) + \alpha \sum_{n=1}^2 z'_n \log(P_n) \quad (3)$$

where z_k is a binary variable indicating whether the k^{th} intent is true, and p_k is the predicted probability of the k^{th} intent. z'_n and P_n are respectively the ground truth and the predicted probability of each class in SUID. α is a down-weighting coefficient.

Similarly, the max-margin loss for capsule networks is:

$$\begin{aligned} \mathcal{L}_{margin} = & \sum_{k=1}^K \left\{ T_k \cdot \max(0, m^+ - \|\mathbf{v}_k\|)^2 \right. \\ & \left. + \lambda(1 - T_k) \cdot \max(0, \|\mathbf{v}_k\| - m^-)^2 \right\} \\ & + \lambda' \sum_{n=1}^2 \left\{ T'_n \cdot \max(0, m'^+ - P_n)^2 \right. \\ & \left. + \lambda(1 - T'_n) \cdot \max(0, P_n - m'^-)^2 \right\} \end{aligned} \quad (4)$$

where $T_k = 1$ when the k^{th} intent is ground-truth, and otherwise $T_k = 0$. T'_n is defined in the same way for SUID. λ and λ' are the down-weighting coefficients, m^+ , m^- and m'^+ , m'^- are the margins. In addition, a regularization term is added to \mathcal{L}_{margin} to encourage the discrepancy among attention heads (Xia et al. 2018).

Similarity Scorer Similarity Scorer, which measures the connections between intent classes, is a key component for transformation-based methods. To compute the inter-intent similarity, we first need to obtain the intent representations. Inspired by Chao et al. (2016), we average the representations of all utterances to represent the seen intents. For the unseen intents, we use the representations of label names. The representation of each utterance or label name is obtained by averaging over different attention heads (for IntentCapsNet) or time steps (for other models). In practice, the representations are computed during the last training epoch, which considers the entire training set (i.e., the parameters of feature extractors are updated in this process).

After the averaging operation, we have the intent representations $\{\mathbf{g}_1, \mathbf{g}_2, \dots, \mathbf{g}_K\} \in \mathbb{R}^{K \times D_H}$, which is used to compute the similarity matrices $\mathbf{L}_{zsl} \in \mathbb{R}^{K \times J}$ for ZSID and $\mathbf{L}_{gzsl} \in \mathbb{R}^{K \times K}$ for GZSID. The similarity between intent k_1 and intent k_2 is computed as:

$$L_{k_1 k_2} = (\mathbf{g}_{k_1} - \mathbf{g}_{k_2})^T \boldsymbol{\Sigma}^{-1} (\mathbf{g}_{k_1} - \mathbf{g}_{k_2}) \quad (5)$$

where $\mathbf{g}_{k_1}, \mathbf{g}_{k_2}$ are the representations of k_1 and k_2 , respectively. $\boldsymbol{\Sigma} = \sigma^2 \mathbf{I}$ models the correlations among intent representation dimensions, where σ is a hyper-parameter.

Inference Process During inference, a test utterance is first encoded into a prediction vector of K dimensions, in the same way as the training process. Based on this vector, we further employ the Similarity Scorer to obtain the final prediction. In terms of the linear classifier, we have:

$$\mathbf{v}_{tr} = \text{Softmax}\left(\frac{1}{T} \sum_{t=1:T} \mathbf{h}_t\right) \mathbf{W} \mathbf{L} \quad (6)$$

where \mathbf{L} refers to \mathbf{L}_{zsl} or \mathbf{L}_{gzsl} . When it comes to the capsule networks:

$$\mathbf{s}_j = \sum_r^R L_{jk} (c_{kr} \hat{\mathbf{u}}_{j|k}) \quad (7)$$

where L_{jk} is the k^{th} entry in the j^{th} row of \mathbf{L} . After Dynamic Routing, we can get J activation vectors for ZSID and K activation vectors for GZSID.

Compatibility-based Methods

Feature Extractor Similar to the transformation-based methods, the first step of compatibility-based methods is to encode the utterance or label name into a dense vector. In this paper we study two kinds of compatibility-based methods: Zero-shotDNN (Kumar et al. 2017) and CDSSM (Chen, Hakkani-Tür, and He 2016). Zero-shotDNN extracts the text representation with a mean pooling of word embeddings and a tanh-activated nonlinear layer. CDSSM uses CNN as the feature extractor, which is followed by a number of max pooling and nonlinear projection operations.

Intent Classifier With the utterance representation and the representations of label names, compatibility-based methods compute the cosine similarity between the utterance u and each intent, which results in $\mathbf{S} = \{sim(u, y) | y \in Y_{seen} \cup Y_{unseen}\} \in \mathbb{R}^K$. Then, u can be classified into a particular intent class according to:

$$\mathbf{v}_{tr} = \text{Softmax}(\mathbf{S}) \quad (8)$$

Multi-task Learning Objective To perform SUID with the compatibility-based classifier, we sum up the first I and last J positions in \mathbf{S} as $\sum_{i=1:I} \mathbf{S}_i$ and $\sum_{i=I+1:K} \mathbf{S}_i$, the result of which is passed to a binary softmax function to obtain the final probabilities for y_{seen} and y_{unseen} . The multi-task learning objective is then formulated as:

$$\mathcal{L}_{compti} = \mathcal{L}_{intcls} + \alpha \sum_{n=1}^2 z_n \log(P_n) \quad (9)$$

where \mathcal{L}_{intcls} is the loss for intent classification. CDSSM adopts the traditional cross-entropy loss as \mathcal{L}_{intcls} , while Zero-shotDNN utilizes a margin-based objective function. α , z_n and P_n are defined in the same way as Equation 3.

Inference Process The inference process for compatibility-based methods is basically the same as the classification process during training. Given an input utterance from unseen intents (ZSID) or either seen or unseen intents (GZSID), we compute its similarity with each candidate intent in the learned representation space, and classify it to the most similar intent.

Two-stage GZSDI Method

In two-stage GZSID method, a test utterance is first classified into one of the class from $Y_{seen} \cup \{y_{unseen}\}$ using the UID classifier. In practice, we use the density-based algorithm LOF (Lin and Xu 2019) to perform UID. The second stage is the task of ZSID, which is performed using the transformation-based or compatibility-based methods as described above.

Experiments

Datasets

We conduct experiments on two benchmarks for intent detection. The detailed statistics are shown in Table 1. **SNIPS** (Coucke et al. 2018) is a corpus to benchmark the performance of voice assistants, which contains 5 seen intents and 2 unseen intents that are pre-defined. **CLINC** (Larson et al.

Dataset	SNIPS	CLINC
Vocabulary	10,896	6,437
Number of Samples	13,802	9,000
Average Sentence Length	9.05	8.34
Average Label Length	2.43	2.07
Number of existing Intents	5	50
Number of emerging Intents	2	10

Table 1: Dataset statistics

2019) includes out-of-scope queries and 22,500 in-scope queries covering 150 intent classes from 10 domains. We only use the in-scope data to build our dataset with 50 seen intents and 10 unseen intents. We select the unseen intents to make sure that there are no predicate overlap between different intent names. Among the unseen intent names only 1/3 words appear in the seen intent names (see Appendix B).

Dataset Processing For ZSID, we use all utterances from seen intents to construct the training set and those from unseen intents to construct the test set. For GZSID, we randomly select 70% utterances of each seen intent for the training set. Although our focus is the zero-shot problem, utterances from seen intents still account for the majority in real-world applications. In light of this phenomenon, we balance the sample number of unseen and seen classes to build the test set: selecting the remaining 30% utterances of each seen intent and 30% random utterances of each unseen intent. To build the unseen training data, we replicate the label names to roughly the same number of the seen utterances.

Experimental Setup

We use the test set performance for hyper-parameter tuning, which is the same with most existing ZSID work. For the SNIPS dataset, we adopt the settings of the original papers to report the baseline results, which perform well. For CLINC dataset, we optimize the baselines as our method, which outperforms the original settings. We run the experiments for five times with different random seeds. Details of the experimental setup are presented in Appendix C.

Evaluation Metrics Four evaluation metrics are considered in our evaluations: Accuracy (Acc), Precision (Pre), Recall (Rec) and F1, all of which are computed with the average value weighted by their support on each class (micro average). Therefore, Rec and Acc are exactly the same.

Baselines

We integrate DIR with representative ZSID systems. For transformation-based methods with linear classifier, we explore the use of CNN (LeCun et al. 1989), uni-directional LSTM (Hochreiter and Schmidhuber 1997), and BERT (Devlin et al. 2019) as the feature extractor, which are denoted as CNN, LSTM and BERT, respectively. We find that use BERT to compute the similarity matrix leads to poor results, as the label names are very short. Therefore, we combine BERT feature extractor with CNN-DIR computed similarity

Model	SNIPS		CLINC	
	Acc/Rec	F1	Acc/Rec	F1
LSTM (Ours)	79.47	79.18	71.73	68.73
+DIR	93.43	93.42	84.48	84.35
CNN (Ours)	65.15	60.91	73.03	70.94
+DIR	94.73	94.73	85.11	85.20
BERT (Ours)	73.66	73.32	62.73	59.45
+DIR	96.13	96.12	88.72	88.45
CDSSM (Chen et al. 2016)	68.98	66.52	64.80	61.14
+key	83.03	82.86	-	-
+DIR	94.14	94.14	83.07	82.52
ZSDNN (Kumar et al. 2017)	80.96	80.74	82.20	82.18
+key	93.49	93.49	-	-
+DIR	95.07	95.07	93.57	93.62
CapsNet (Xia et al. 2018)	74.21	72.58	64.51	61.87
+key	93.49	93.49	-	-
+DIR	94.84	94.84	87.01	86.91

Table 2: Results of ZSID.

matrix for the BERT baseline. For capsule network classifier, we select IntentCapsNet (Xia et al. 2018) as the baseline system. In terms of the compatibility-based methods, we study the effect of DIR on Zero-shotDNN (Kumar et al. 2017) and CDSSM (Chen, Hakkani-Tür, and He 2016).

We also introduce two strong baselines targeting the two limitations discussed in the Introduction. For the intent relationship problem, we replace the original label names with manually selected keywords in the ZSID setting (denoted as + key). For the domain-shift problem in GZSID, we follow Yan et al. (2020) to build a two-stage approach. In the first stage we use the SOTA method LOF (LMCL) (Lin and Xu 2019) to perform the UID, and the second stage of ZSID is accomplished by the baseline methods (denoted as + LOF). We follow the code released by Lin and Xu (2019) to train the first stage UID model.

ReCapsNet (Liu et al. 2019) and the two-stage method with SEG (Yan et al. 2020), which achieve the SOTA performance, are not open-sourced. To compare with them, we run our method on their setting: They build the GZSID test set with 30% seen intent utterances and all unseen intent utterance. As we have discussed, seen intents still account for the majority in real-world application, and therefore 30% seen versus all unseen underestimates the importance of seen intents. The label names used by these work are also slightly different from our main experiments, as we use the raw label names without modification.

Results

Performance in ZSID The ZSID results are reported in Table 2. As we can see, the performance of CDSSM, ZSDNN and CapsNet can be significantly improved with the manually composed keyword labels. This demonstrates the first limitation that existing ZSID methods are not good at associating the relationship between seen and unseen intents when the label names are given in raw phrases or sentences. Our proposed framework, regardless of the backbone network and ZSID strategy, consistently outperforms the baselines with comfortable margin (11.49 ~ 33.82 absolute F1 improvement). More importantly, the DIR-enhanced models

Model	SNIPS						CLINC					
	Seen		Unseen		Overall		Seen		Unseen		Overall	
	Acc	F1	Acc	F1	Acc	F1	Acc	F1	Acc	F1	Acc	F1
LSTM (Ours)	97.22	83.94	0.00	0.00	69.66	60.14	93.19	85.95	0.00	0.00	77.65	71.62
+DIR	95.42	86.00	31.34	45.32	77.26	74.47	93.40	87.55	20.50	30.96	81.24	78.12
CNN (Ours)	97.95	85.09	0.00	0.00	70.18	60.97	95.35	87.89	0.00	0.00	79.46	73.24
+DIR	96.59	88.41	46.22	62.37	82.31	81.03	96.25	90.06	15.82	23.11	82.85	78.91
BERT (Ours)	96.43	84.70	0.00	0.00	69.1	60.69	88.14	82.17	0.23	0.44	73.49	68.55
+DIR	96.93	89.62	49.38	61.15	83.45	81.55	97.84	91.19	12.55	19.74	83.62	79.29
CDSSM (Chen et al. 2016)	97.99	84.54	0.19	0.37	70.32	60.74	93.62	86.66	2.09	3.69	78.35	72.82
+LOF	81.52	88.22	60.75	49.14	75.63	77.14	79.96	86.94	42.80	28.96	73.76	77.28
+DIR	92.55	84.63	42.91	56.46	78.51	76.66	94.72	89.11	23.64	32.39	82.87	79.65
+LOF+DIR	81.52	88.22	87.00	73.01	83.08	83.90	79.96	86.94	61.32	44.58	76.89	79.97
ZSDNN (Kumar et al. 2017)	94.79	83.29	10.50	17.40	70.93	64.64	85.45	81.14	26.79	36.07	75.63	73.73
+LOF	81.52	88.22	66.37	55.24	77.23	78.86	79.96	86.94	64.04	47.13	77.30	80.30
+DIR	95.82	89.11	58.03	73.00	85.12	84.55	91.75	88.18	47.15	58.69	84.30	83.18
+LOF+DIR	81.52	88.22	88.52	74.30	83.51	84.27	79.96	86.94	75.47	54.80	79.21	81.85
CapsNet (Xia et al. 2018)	97.99	84.34	0.00	0.00	70.22	60.43	97.92	90.31	0.23	0.42	81.64	75.33
+LOF	81.52	88.22	64.74	53.00	76.76	78.23	79.96	86.94	46.04	33.80	74.30	78.08
+DIR	97.47	89.15	47.17	63.90	83.21	81.99	97.71	92.29	30.95	43.09	86.58	84.09
+LOF+DIR	81.52	88.22	86.63	72.91	82.97	83.88	79.96	86.94	64.40	46.76	77.36	80.24

Table 3: Results of GZSID. CpasNet and ZSDNN are short for IntentCapsNet and Zero-shotDNN respectively.

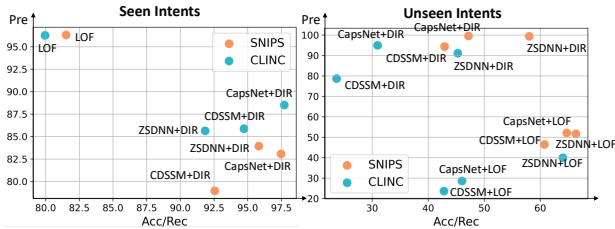


Figure 2: Trade-off between Pre and Acc/Rec. We only have one LOF result each dataset for seen intents because the three systems use the same LOF model in the first stage. Appendix D shows the per class result regarding this effect.

also achieve better results than the manually selected keywords, with an encouraging improvement of 11.28 F1 score for the CDSSM baseline. This shows the effectiveness of the proposed method to alleviate the effect of poor quality label names, dispensing with the need of manual modification. We find that our experiment results of CapsNet is different from those reported by Xia et al. (2018). The reason is that we use the original intent labels to compute similarity.

Performance in GZSID From the results in Table 3, we can derive five observations: First, the baselines work well on the seen intents, while they fail to detect the unseen intents. This phenomenon attests to the second limitation2 that the ZSID systems cannot effectively work in the GZSID scenario. Second, the two-stage framework (+LOF) brings significant improvement on the unseen intents, successfully alleviating the domain-shift problem. Third, our DIR framework improves the performance to a larger extent, which on average outperforms +LOF with 10.04 F1 on unseen intents and 3.37 F1 in terms of overall performance.

An advantage of DIR over +LOF is that the two-stage

Model	ZSID		GZSID	
	Acc/Rec	F1	Acc/Rec	F1
ReCapsNet (Liu et al. 2019)	79.96	79.80	47.05	38.26
SEG (Yan et al. 2020)	-	-	76.85	76.74
ZSDNN+DIR	95.05	95.05	74.41	75.44
ZSDNN+LOF	-	-	76.93	77.07
CapsNet+LOF+DIR	-	-	82.90	83.19
ZSDNN+LOF+DIR	-	-	84.10	84.33

Table 4: Comparison with SOTA methods in SNIPS.

method increases the Acc/Rec on unseen intents at the cost of Acc/Rec on seen intents, while DIR maintains the seen Acc/Rec to the same level as the baselines (sometimes even better). This leads to another finding. As Figure 2 shows, +LOF and DIR reveal a trade-off between Pre and Acc/Rec. +LOF recalls more unseen intent utterances but at the same time mistakenly classifies some seen intent utterances into *y_{unseen}*, which hurts Pre on unseen intents and Acc/Rec on seen intents. By contrast, DIR classifies less utterances to the unseen classes, but at higher precision. Meanwhile, the Acc/Rec on seen intents obvious outstrips +LOF.

Finally, DIR can further promote the strong two-stage baseline: Enhancing the second stage ZSID model with DIR (+LOF+DIR) results in a substantial improvement of +LOF on the unseen intents, where the Acc/Rec is increased by 19.77 on average and F1 score is increased by 16.52 on average. The overall performance is thereby also improved.

Comparison with SOTA methods Table 4 presents the comparison of the proposal with SOTA methods under their experimental settings as described in the Baselines. As we can see, the +LOF+DIR methods clearly outperforms the current SOTAs in both ZSID and GZSID. The +DIR method is comparable with SEG in GZSID. One may find that ZSDNN+LOF+DIR is better than ZSDNN+DIR in Table 4,

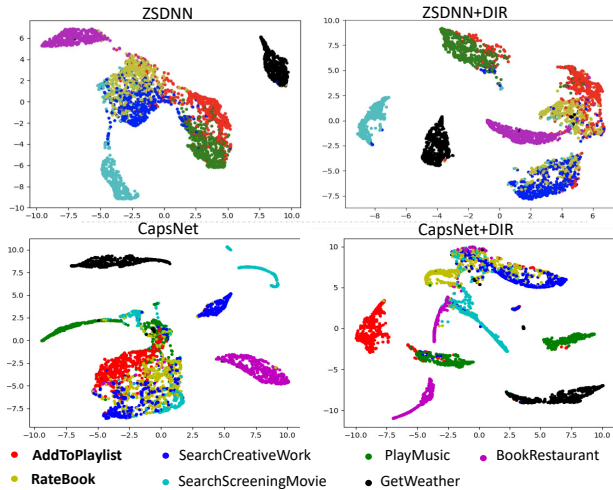


Figure 3: Data visualization on SNIP test set. “AddToPlaylist” and “RateBook” are the unseen intents.

Model	SNIPS				CLINC			
	ZSID		GZSID		ZSID		GZSID	
	Acc	F1	Acc	F1	Acc	F1	Acc	F1
CNN + DIR	94.73	94.73	82.31	81.03	85.11	85.20	82.91	78.88
w/o MT	94.09	94.08	82.24	80.96	84.96	85.01	82.85	78.73
w/o SS	94.54	94.53	80.55	79.60	83.78	83.82	84.24	80.25
SS → ES	81.89	80.95	80.51	79.50	82.44	82.54	82.54	78.29
CapsNet + DIR	94.84	94.84	83.21	81.99	87.01	86.91	86.58	84.09
w/o MT	93.68	93.67	81.02	79.07	85.17	85.07	86.19	83.64
w/o SS	90.30	90.26	83.20	81.94	85.37	85.16	86.26	83.69
SS → ES	82.54	81.96	83.11	81.90	79.97	79.79	86.57	83.92
ZSDNN + DIR	95.07	95.07	85.12	84.55	93.57	93.62	84.30	83.18
w/o MT	93.55	93.52	84.90	84.30	93.40	93.46	84.03	82.81
CDSSM + DIR	94.14	94.14	78.51	76.66	83.07	82.52	82.87	79.65
w/o MT	93.84	93.83	78.73	76.01	82.68	82.12	82.79	79.57

Table 5: Results of ablation study. w/o MT and w/o SS indicate removing multi-task learning and the similarity scorer, respectively. SS → ES means replacing our Similarity Scorer with the word embedding based similarity.

while lags behind in our GZSID setting. The reason is that their dataset splitting assigns less importance to the seen intents, where DIR performs better than the two-stage method.

Ablation Study

Table 5 shows the results of ablation study. We can observe that: 1) Our similarity scorer clearly outperforms the word embedding based intent similarity (please refer to Appendix A for a qualitative comparison of the similarity matrices), especially in the ZSID setting. The advantage of SS over ES is less obvious in GZSID because the model trained with DIR can directly perform GZSID, which makes the effect of the similarity matrix less significant. This can also explain for the phenomenon that w/o SS outperforms CNN+DIR in CLINC under GZSID setting. 2) In spite of this, removing the similarity scorer has a negative impact on the model performance. 3) Multi-task learning consistently benefits the DIR framework in all circumstances. For GZSID, the improvement directly comes from the disentangling effect of MT. For ZSID, we attribute the improvement to the well-learned relationship between seen and unseen intents, which

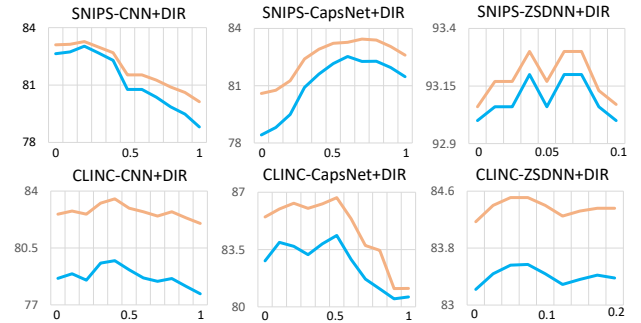


Figure 4: Overall GZSID ACC (orange) and F1 (blue) with the variation of down-weighting coefficients.

is a side-effect of the disentangled representations.

The Effect of Down-Weighting Coefficients

As shown in Figure 4, the performance varies with the increase of α and λ' . For different models and datasets, the comfortable region is different, but generally, the scores first increases and then declines. This suggests that distinguishing seen and unseen intent is beneficial but paying too much attention to this objective can hurt the final performance.

Visualization

To examine whether the DIR framework can actually learn disentangled intent representations, we visualize the utterance representations using the feature extractors of four methods (see Figure 3). Please focus on the two unseen intents. We can see that the two unseen intents “AddToPlaylist” (red) and “RateBook” (yellow) are entangled with “SearchCreativeWork” (blue) and “PlayMusic” (green) in the CapsNet representation space. For ZSDNN representations, yellow dots and blue dots appear as a single cluster, so it is with red dots and green dots. These entangled representations make it difficult to perform GZSID. In comparison, the CapsNet+DIR successfully learns an independent subspace for “AddToPlaylist” and disentangles a part of “RateBook” from the seen intents. ZSDNN+DIR pulls the two unseen classes as a whole out from the seen classes, with a vague but identifiable boundary in between.

Conclusions

In this paper, we propose a class-transductive framework to overcome the limitations of existing ZSID models. The framework learns disentangled representations for unseen intents by including them into the prediction space during training. Under the DIR framework, we present a multi-task learning objective in the training stage to encourages the model to learn the distinctions between unseen and seen intents. In the inference stage, we develop a similarity scorer, which can better associate the inter-intent connections based on the learned representations. Experiments on two benchmarks show that DIR is effective and robust, which can bring considerable improvement to ZSID systems with different zero-shot learning strategies and backbone networks.

References

- Bojanowski, P.; Grave, E.; Joulin, A.; and Mikolov, T. 2017. Enriching word vectors with subword information. *Transactions of the Association for Computational Linguistics* 5: 135–146.
- Chao, W.-L.; Changpinyo, S.; Gong, B.; and Sha, F. 2016. An empirical study and analysis of generalized zero-shot learning for object recognition in the wild. In *European Conference on Computer Vision*, 52–68. Springer.
- Chen, Y.-N.; Hakkani-Tür, D.; and He, X. 2016. Zero-shot learning of intent embeddings for expansion by convolutional deep structured semantic models. In *2016 IEEE International Conference on Acoustics, Speech and Signal Processing (ICASSP)*, 6045–6049. IEEE.
- Chen, Y.-N.; Hakkani-Tür, D.; Tür, G.; Gao, J.; and Deng, L. 2016. End-to-end memory networks with knowledge carryover for multi-turn spoken language understanding. In *Interspeech*, 3245–3249.
- Coucke, A.; Saade, A.; Ball, A.; Bluche, T.; Caulier, A.; Leroy, D.; Doumouro, C.; Gisselbrecht, T.; Caltagirone, F.; Lavril, T.; et al. 2018. Snips voice platform: an embedded spoken language understanding system for private-by-design voice interfaces. *arXiv preprint arXiv:1805.10190*.
- Devlin, J.; Chang, M.; Lee, K.; and Toutanova, K. 2019. BERT: Pre-training of Deep Bidirectional Transformers for Language Understanding. In *NAACL-HLT (1)*, 4171–4186. Association for Computational Linguistics.
- Elhoseiny, M.; Saleh, B.; and Elgammal, A. M. 2013. Write a Classifier: Zero-Shot Learning Using Purely Textual Descriptions. In *ICCV*, 2584–2591. IEEE Computer Society.
- Farhadi, A.; Endres, I.; Hoiem, D.; and Forsyth, D. 2009. Describing objects by their attributes. In *2009 IEEE Conference on Computer Vision and Pattern Recognition*, 1778–1785. IEEE.
- Ferreira, E.; Jabaian, B.; and Lefevre, F. 2015. Online adaptive zero-shot learning spoken language understanding using word-embedding. In *2015 IEEE International Conference on Acoustics, Speech and Signal Processing (ICASSP)*, 5321–5325. IEEE.
- Ferreira, E.; Jabaian, B.; and Lefèvre, F. 2015. Zero-shot semantic parser for spoken language understanding. In *Sixteenth Annual Conference of the International Speech Communication Association*.
- Frome, A.; Corrado, G. S.; Shlens, J.; Bengio, S.; Dean, J.; Ranzato, M.; and Mikolov, T. 2013. Devise: A deep visual-semantic embedding model. In *Advances in neural information processing systems*, 2121–2129.
- Fu, Y.; Hospedales, T. M.; Xiang, T.; and Gong, S. 2015a. Transductive multi-view zero-shot learning. *IEEE transactions on pattern analysis and machine intelligence* 37(11): 2332–2345.
- Fu, Z.; Xiang, T.; Kodirov, E.; and Gong, S. 2018. Zero-Shot Learning on Semantic Class Prototype Graph. *IEEE Trans. Pattern Anal. Mach. Intell.* 40(8): 2009–2022.
- Fu, Z.; Xiang, T. A.; Kodirov, E.; and Gong, S. 2015b. Zero-shot object recognition by semantic manifold distance. In *CVPR*, 2635–2644. IEEE Computer Society.
- Haihong, E.; Niu, P.; Chen, Z.; and Song, M. 2019. A novel bi-directional interrelated model for joint intent detection and slot filling. In *Proceedings of the 57th Annual Meeting of the Association for Computational Linguistics*, 5467–5471.
- Hochreiter, S.; and Schmidhuber, J. 1997. Long short-term memory. *Neural computation* 9(8): 1735–1780.
- Hu, J.; Wang, G.; Lochovsky, F.; Sun, J.-t.; and Chen, Z. 2009. Understanding user’s query intent with wikipedia. In *Proceedings of the 18th international conference on World wide web*, 471–480.
- Kumar, A.; Muddireddy, P. R.; Dreyer, M.; and Hoffmeister, B. 2017. Zero-Shot Learning Across Heterogeneous Overlapping Domains. In *INTERSPEECH*, 2914–2918.
- Lampert, C. H.; Nickisch, H.; and Harmeling, S. 2009. Learning to detect unseen object classes by between-class attribute transfer. In *CVPR*, 951–958. IEEE Computer Society.
- Larson, S.; Mahendran, A.; Peper, J. J.; Clarke, C.; Lee, A.; Hill, P.; Kummerfeld, J. K.; Leach, K.; Laurenzano, M. A.; Tang, L.; and Mars, J. 2019. An Evaluation Dataset for Intent Classification and Out-of-Scope Prediction. In *EMNLP/IJCNLP (1)*, 1311–1316. Association for Computational Linguistics.
- LeCun, Y.; Boser, B.; Denker, J. S.; Henderson, D.; Howard, R. E.; Hubbard, W.; and Jackel, L. D. 1989. Backpropagation applied to handwritten zip code recognition. *Neural computation* 1(4): 541–551.
- Lin, T.; and Xu, H. 2019. Deep Unknown Intent Detection with Margin Loss. In *ACL (1)*, 5491–5496. Association for Computational Linguistics.
- Lin, Z.; Feng, M.; dos Santos, C. N.; Yu, M.; Xiang, B.; Zhou, B.; and Bengio, Y. 2017. A Structured Self-Attentive Sentence Embedding. In *ICLR (Poster)*. OpenReview.net.
- Liu, B.; and Lane, I. 2016. Attention-Based Recurrent Neural Network Models for Joint Intent Detection and Slot Filling. In *INTERSPEECH*, 685–689. ISCA.
- Liu, H.; Zhang, X.; Fan, L.; Fu, X.; Li, Q.; Wu, X.-M.; and Lam, A. Y. 2019. Reconstructing Capsule Networks for Zero-shot Intent Classification. In *Proceedings of the 2019 Conference on Empirical Methods in Natural Language Processing and the 9th International Joint Conference on Natural Language Processing (EMNLP-IJCNLP)*, 4801–4811.
- Mensink, T.; Verbeek, J.; Perronnin, F.; and Csurka, G. 2012. Metric learning for large scale image classification: Generalizing to new classes at near-zero cost. In *European Conference on Computer Vision*, 488–501. Springer.
- Mikolov, T.; Chen, K.; Corrado, G.; and Dean, J. 2013. Efficient Estimation of Word Representations in Vector Space. In *ICLR (Workshop Poster)*.

- Nam, J.; Mencía, E. L.; and Fürnkranz, J. 2016. All-in text: Learning document, label, and word representations jointly. In *Thirtieth AAAI Conference on Artificial Intelligence*.
- Norouzi, M.; Mikolov, T.; Bengio, S.; Singer, Y.; Shlens, J.; Frome, A.; Corrado, G.; and Dean, J. 2014. Zero-Shot Learning by Convex Combination of Semantic Embeddings. In *ICLR*.
- Parikh, D.; and Grauman, K. 2011. Relative attributes. In *2011 International Conference on Computer Vision*, 503–510. IEEE.
- Pennington, J.; Socher, R.; and Manning, C. D. 2014. Glove: Global vectors for word representation. In *Proceedings of the 2014 conference on empirical methods in natural language processing (EMNLP)*, 1532–1543.
- Ravuri, S.; and Stolcke, A. 2015. Recurrent neural network and LSTM models for lexical utterance classification. In *Sixteenth Annual Conference of the International Speech Communication Association*.
- Sabour, S.; Frosst, N.; and Hinton, G. E. 2017. Dynamic routing between capsules. In *Advances in neural information processing systems*, 3856–3866.
- Scheirer, W. J.; de Rezende Rocha, A.; Sapkota, A.; and Boulton, T. E. 2012. Toward open set recognition. *IEEE transactions on pattern analysis and machine intelligence* 35(7): 1757–1772.
- Schuster, M.; and Paliwal, K. K. 1997. Bidirectional recurrent neural networks. *IEEE transactions on Signal Processing* 45(11): 2673–2681.
- Socher, R.; Ganjoo, M.; Manning, C. D.; and Ng, A. 2013. Zero-shot learning through cross-modal transfer. In *Advances in neural information processing systems*, 935–943.
- Tur, G.; Deng, L.; Hakkani-Tür, D.; and He, X. 2012. Towards deeper understanding: Deep convex networks for semantic utterance classification. In *2012 IEEE international conference on acoustics, speech and signal processing (ICASSP)*, 5045–5048. IEEE.
- Vaswani, A.; Shazeer, N.; Parmar, N.; Uszkoreit, J.; Jones, L.; Gomez, A. N.; Kaiser, Ł.; and Polosukhin, I. 2017. Attention is all you need. In *Advances in neural information processing systems*, 5998–6008.
- Wang, W.; Zheng, V. W.; Yu, H.; and Miao, C. 2019. A Survey of Zero-Shot Learning: Settings, Methods, and Applications. *ACM Trans. Intell. Syst. Technol.* 10(2): 13:1–13:37.
- Wang, X.; Ye, Y.; and Gupta, A. 2018. Zero-Shot Recognition via Semantic Embeddings and Knowledge Graphs. In *CVPR*, 6857–6866. IEEE Computer Society.
- Xia, C.; Zhang, C.; Yan, X.; Chang, Y.; and Yu, P. S. 2018. Zero-shot User Intent Detection via Capsule Neural Networks. In *EMNLP*, 3090–3099. Association for Computational Linguistics.
- Xian, Y.; Lampert, C. H.; Schiele, B.; and Akata, Z. 2019. Zero-Shot Learning - A Comprehensive Evaluation of the Good, the Bad and the Ugly. *IEEE Trans. Pattern Anal. Mach. Intell.* 41(9): 2251–2265.
- Xu, P.; and Sarikaya, R. 2013. Convolutional neural network based triangular crf for joint intent detection and slot filling. In *2013 IEEE workshop on automatic speech recognition and understanding*, 78–83. IEEE.
- Yan, G.; Fan, L.; Li, Q.; Liu, H.; Zhang, X.; Wu, X.; and Lam, A. Y. S. 2020. Unknown Intent Detection Using Gaussian Mixture Model with an Application to Zero-shot Intent Classification. In *ACL*, 1050–1060. Association for Computational Linguistics.
- Yazdani, M.; and Henderson, J. 2015. A model of zero-shot learning of spoken language understanding. In *Proceedings of the 2015 Conference on Empirical Methods in Natural Language Processing*, 244–249.
- Zhang, C.; Fan, W.; Du, N.; and Yu, P. S. 2016a. Mining user intentions from medical queries: A neural network based heterogeneous jointly modeling approach. In *Proceedings of the 25th International Conference on World wide web*, 1373–1384.
- Zhang, C.; Li, Y.; Du, N.; Fan, W.; and Yu, P. S. 2019. Joint Slot Filling and Intent Detection via Capsule Neural Networks. In *ACL (1)*, 5259–5267. Association for Computational Linguistics.
- Zhang, H.; Shang, X.; Yang, W.; Xu, H.; Luan, H.; and Chua, T.-S. 2016b. Online collaborative learning for open-vocabulary visual classifiers. In *Proceedings of the IEEE conference on computer vision and pattern recognition*, 2809–2817.
- Zhang, J.; Lertvittayakumjorn, P.; and Guo, Y. 2019. Integrating Semantic Knowledge to Tackle Zero-shot Text Classification. In *NAACL-HLT (1)*, 1031–1040. Association for Computational Linguistics.